Chapter

# Hybrid Modeling Procedure of Li-Ion Battery Modules for Reproducing Wide Frequency Applications in Electric Systems

*Sandra Castano-Solis, Daniel Serrano-Jiménez, Jesús Fraile-Ardanuy, David Jiménez-Bermejo and Javier Sanz-Feito*

## Abstract

In this chapter, a hybrid modeling procedure of Li-ion battery modules is presented. From experimental results, the parameters of an electrical circuit have been determined by means of time- and frequency-domain tests. In this way, the dynamic behavior of the battery-pack is modeled. The tests have been performed at the whole battery-pack, instead of a single-cell approach, in order to consider the packaging effects of multicell devices. The real performance of the battery-pack under dynamic applications associated with distribution grids has been simulated using a hardware-in-the-loop (HIL) experimental setup. According to simulation results, the hybrid model follows the battery-pack response with high accuracy.

**Keywords:** battery-pack modeling, dynamic performance electric grids, time-domain test, frequency-domain tests, HIL simulations

## 1. Introduction

Introducing renewable energy sources such as photovoltaic generators and wind turbines into energy distribution grids presents some drawbacks because the energy generation is discontinuous and strongly depends on daily weather conditions. For these reasons, distribution grids with high penetration of renewable resources present problems of reliability, stability, and power quality [1]. To solve these issues, several researchers recommend energy storage systems as support systems [2, 3].

In recent years, the improvements in terms of materials, high specific energy and power, and long life cycle have made Li-based batteries as a viable option to reduce renewable generation interruptions [4]. Because the nominal voltage of Li-ion cells is less than 4 V, commercial devices are composed by several Li-ion cells in a combination of series and/or parallel connections, to provide the desired power and capacity of the grid-scale applications. Multicell Li-ion devices include a battery management system (BMS) in order to prevent the cells' voltage, temperature, and charging/discharging current from exceeding the safety limits [5]. Also, the BMS uses algorithms to equalize the cells' voltage to avoid the cells' voltage differences (produced by manufacturing processes and/or ageing processes) from limiting the whole pack performance [6]. Besides electrochemical behavior of Li-ion cells, the performance of the battery-pack is affected by the interactions between cells and BMS components. This configuration increases the nonlinear behavior of commercial battery devices compared with single cells. For all these aforementioned reasons, modeling of battery-packs is a difficult task.

Several battery models have been proposed in literature in order to facilitate their integration into different applications. The most detailed models include electrochemical- or physical-based models, which are able to accurately describe the chemical processes taking place inside battery cells [7, 8]. Despite their accuracy, these models are very complex to be implemented in a simulation tool, and the coupled nonlinear differential equations that compose the model require heavy computational work [9, 10]. In contrast with electrochemical models, electrical circuit models are not very complex, allow the simulation of the electrical response of the battery by using electrical elements (resistances, RC networks, ideal voltage sources, etc.), and can be easily incorporated in control strategies and simulation platforms. The simplest electrical circuit model of a battery is given by Thevenin's equivalent circuit, which is composed of an ideal voltage source in series with a constant internal resistance [11–13]. This model can be used in an initial stage of battery dimensioning, but in the case of dynamic applications, it does not offer information regarding the transient behavior of battery [10, 14].

The accuracy of a battery model depends on the procedure used to obtain its parameters. Modeling techniques can be classified from simple black-box approaches to time- or frequency-domain procedures. Black-box models are simple to obtain, but do not provide information on the battery's internal behavior. Time-domain models are obtained from the analysis of the battery voltage evolution during charge–discharge tests by means of the procedure called current interruption test. In order to improve the model accuracy, some authors [15, 16] use online parameter identification methods to predict battery dynamical behavior as a function of time. These models are relatively easy to obtain, but their validity is usually limited to specific load regimes [17]. Frequency-domain based models are performed by means of electrochemical impedance spectroscopy (EIS) tests [18, 19]. In this technique, a small AC excitation signal (either current or voltage) is applied as a variable frequency sweep to the battery. To obtain a linear model, the amplitude of the AC excitation signal applied to the cell is kept between 5 and 10% of the rated voltage/current. Although EIS models can be time-consuming to obtain, they can reproduce accurate battery behavior in a wide frequency range, typically from mHz to kHz [20, 21]. The equivalent complex impedance is calculated as the quotient between the instantaneous values of voltage and current for each test point.

Li-ion battery-packs are modeled in the majority of the cases as an aggregation of individual cell models, neglecting the packaging effects of multicell devices, although some recent works have shown that considering the interactions between cells and BMS elements can improve the accuracy of the Li-ion battery-packs models [22, 23]. Also, most battery models do not consider that battery modules can work at different dynamic regimes due to internal electrochemical processes that affect their transient behavior. In highly dynamic applications such as electrical grid support or frequency control in microgrids, there are three time constants of special interest [24]. The first one corresponds to the fast processes with dynamic performance from millisecond to seconds, and it is related to safety control of the battery-pack. The second constant refers to the load regime, which produces different charging/discharging cycles of the battery-pack. Finally, ageing processes that occur during long time (months or years) affect the state of charge (SOC) estimation. All these aspects should be taken into account in the modeling procedure of Li-ion battery-packs in order to reproduce their real behavior.

This work presents a hybrid modeling procedure of battery-packs based on time- and frequency-domain tests. From experimental results, the parameters of an electrical circuit are calculated. The elements of the electric circuit are a voltage source, which is determined by current interruption tests (in time domain), and an impedance measured by electrochemical impedance spectroscopy tests (in frequency domain). All tests have been carried out at the whole battery assembly, instead of single-cell measurements, in order to consider the packaging effects of multicell devices. The model has been experimentally validated using hardware-in-the-loop (HIL) simulations. In this way, the battery-pack performance under high dynamic load regimes in distribution grids has been reproduced.

The chapter's contents are organized as follows: Section 2 explains the proposed hybrid model procedure, Section 3 presents the validation tests using a hardware-in-the-loop experimental setup, and finally, in Section 4, the conclusions are presented.

## 2. Hybrid modeling procedure

To reproduce the behavior of Li-ion batteries using an electric circuit, the circuit topology includes a voltage source that represents the active behavior of the battery and a series impedance of the passive one. In the hybrid experimental procedure proposed in this work, the parameters of the electrical model have been calculated from experimental results of both time- and frequency-domain tests.

The modeling procedure is applied to a commercial battery-pack composed of four parallel-connected strings (seven cells connected in series in each string) and a battery management system. BMS functions include measurement of cell voltage, temperature, and current of each series connection, an algorithm for cell voltage balancing, and the disconnection during charging and discharge processes (to avoid cells over/under voltage). **Figure 1** shows a battery-pack connection scheme. The technical data of the battery-pack are presented in **Table 1**.

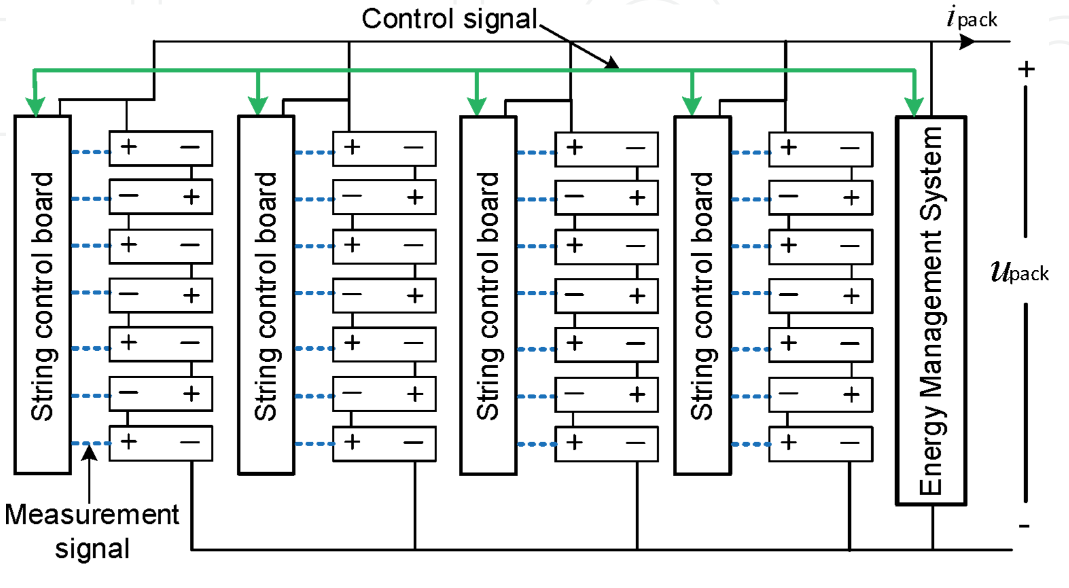


**Figure 1.**
*Battery-pack connections.*

| | |
|---|---|
| Cells reference | MP 176065 Int (Saft batteries) |
| Pack rated voltage | 25.9 V |
| Pack maximum voltage | 29.4 V (4.2 V per cell) |
| Pack minimum cutoff voltage | 20.3 V (2.9 V per cell) |
| Pack capacity, $C_n$ | 50 Ah |
| Pack maximum current | 50 A |
| Range of temperature (charge) | −20 to 60°C |
| Range of temperature (discharge) | −30 to 55°C |

**Table 1.**
*Battery-pack technical data.*

## 2.1 Modeling of the voltage source

To model the voltage source ($E_0$) of the battery-pack, the relationship between the open circuit voltage (OCV) and the state of charge is calculated by means of current interruption tests. First, the battery-pack is totally charged applying the constant current-constant voltage method (25 A until reaching the maximum voltage). After charging process, the device is discharged at current pulses of 10 A for 30 min (0.1 SOC variation) followed by 90 min of relaxation time. The OCV value for each test point is recorded when the relaxation time ends. Finally, the battery-pack is recharged at current pulses of 10 A for 30 min (0.1 SOC variation) followed by 90 min of relaxation time as in the case of discharge process. In the same manner, the OCV values are recorded at the end of the relaxation time. The results of these tests are shown in **Figure 2** (discharging test) and **Figure 3** (charging test). **Table 2** presents the OCV values associated with each SOC test point, and this relationship is also sketched in **Figure 4**. As it can be seen, at the end of charge test, the final value of 100% of SOC is not reached because the BMS limits the applied current during the two last pulses. It is important to highlight that this situation does not occur when a single cell is tested, because the cell is charged and discharged from 100% SOC to 0% SOC without protection of BMS. In addition, test results do not show a high deviation of the average values as is reported in literature [25]; therefore, these values are used to evaluate the OCV-SOC relationship, which is presented in Eq. (1).

$$E_o(SOC, t) = 26.05 - 0.15 \cdot SOC + 3.51 \cdot SOC^2 \tag{1}$$

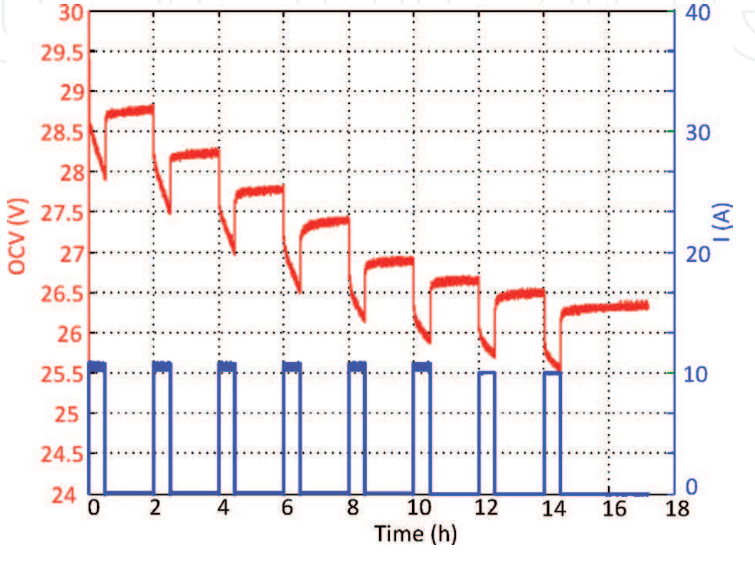


**Figure 2.**
*Discharge test result.*

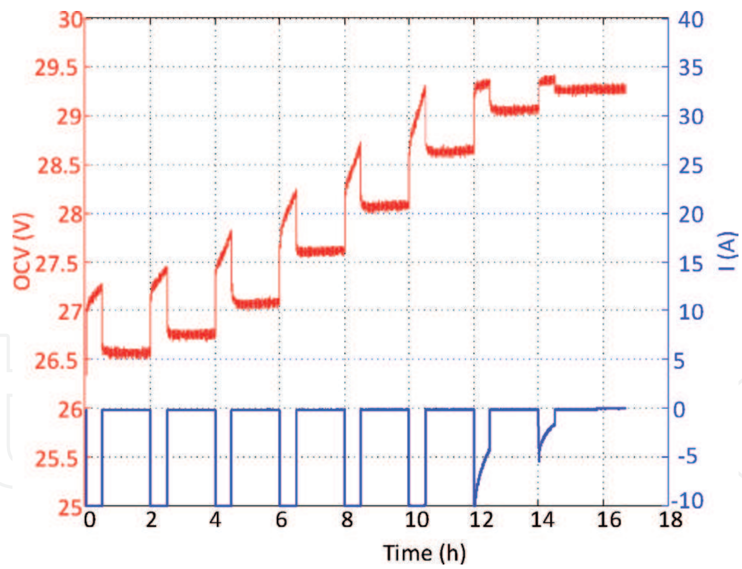


**Figure 3.**
*Charge test result.*

| Discharge results | | Charge results | |
|---|---|---|---|
| **OCV** | **SOC (%)** | **OCV** | **SOC (%)** |
| 29.40 | 100 | 29.28 | 90.27 |
| 28.77 | 90 | 29.06 | 87.64 |
| 28.23 | 80 | 28.65 | 80 |
| 27.79 | 70 | 28.09 | 70 |
| 27.40 | 60 | 27.62 | 60 |
| 26.89 | 50 | 27.08 | 50 |
| 26.65 | 40 | 26.76 | 40 |
| 26.49 | 30 | 26.57 | 30 |
| 26.33 | 20 | 26.33 | 20 |

**Table 2.**
*OCV values at each test point.*

## 2.2 Modeling of the battery-pack's complex impedance

To carry out EIS tests, an impedance analyzer is generally used. This device generates a frequency sweep signal and measures the voltage and current in each test point. As a result, the complex impedance is calculated. Because most of commercial impedance analyzer generates AC signals less than 100 mA (suitable for cell testing), in this work, this signal is amplified and controlled by means of the experimental test bench deeply explained in [26].

EIS tests have been performed at different SOC values (20, 40, 60, 80, and 90% SOC) to analyze the effects of these SOC variations. The frequency sweep has been set from 1 mHz to 5 kHz (typically test range), with an AC ripple of 5 A (10% $I_{max}$). **Figure 5** shows the Nyquist plots of the EIS results, which has been used to analyze the impedance behavior of the tested battery module. In this graph, the real part of the complex impedance (Z') is represented along the x-axis and the imaginary part (Z") along the y-axis. The capacitive behavior corresponds to negative values of Z" and the inductive behavior to the positive ones. In this way, it is easy to identify the parameters of the electrical circuit. According to EIS results, the impedance

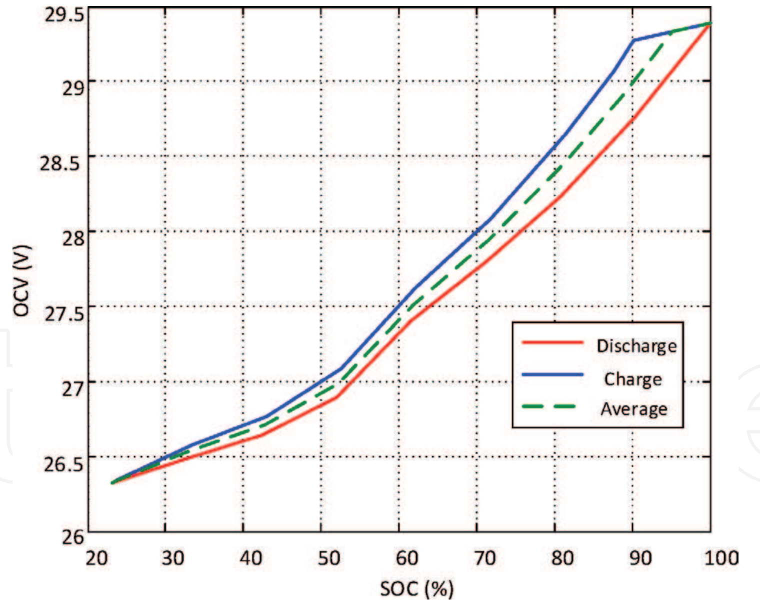


**Figure 4.**
*OCV-SOC characteristic.*

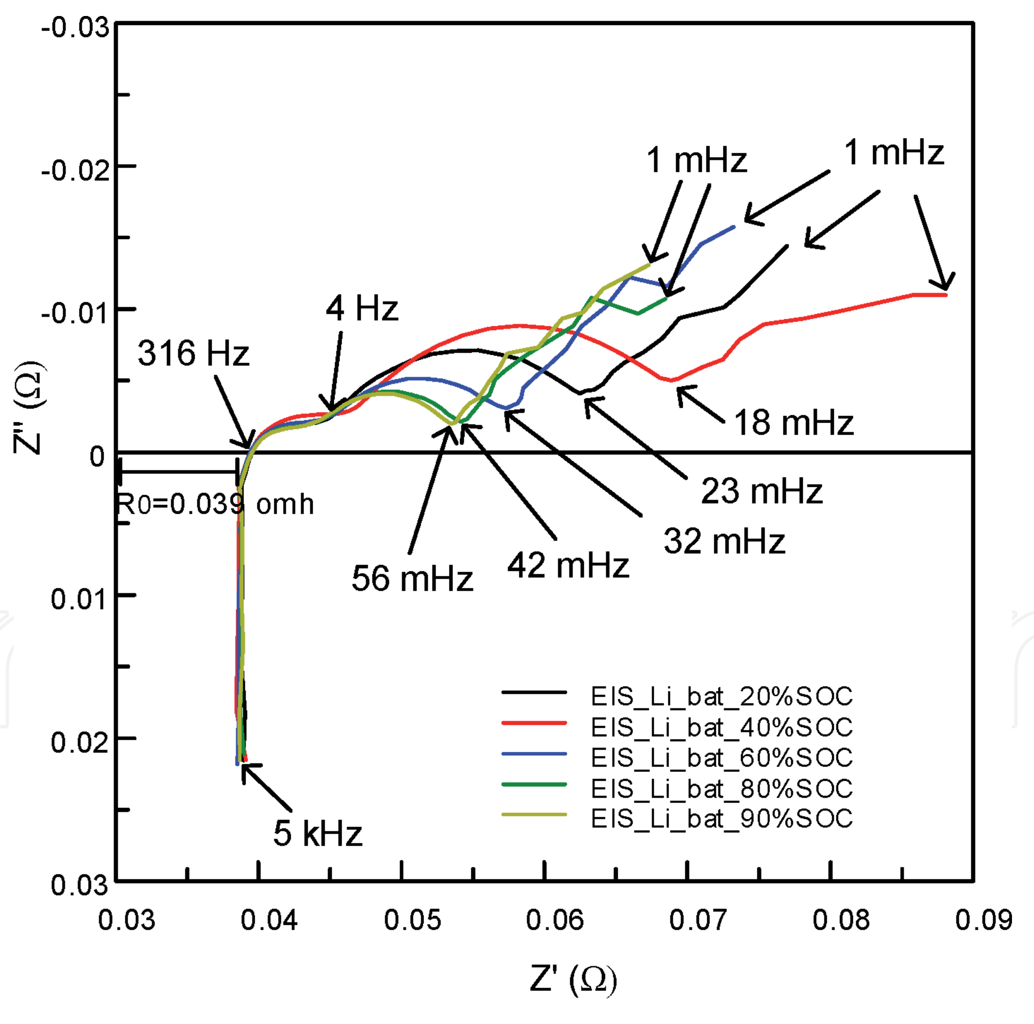


**Figure 5.**
*EIS tests result.*

of the pack tested shows a capacitive behavior from 1 mHz to 316 Hz. From this value, the pack impedance corresponds to an ideal inductance. The differences in these plots reflect that SOC variations affect the capacitive behavior from 1 mHz to 4 Hz. For low frequencies, the Nyquist plots show that both real (Z') and imaginary

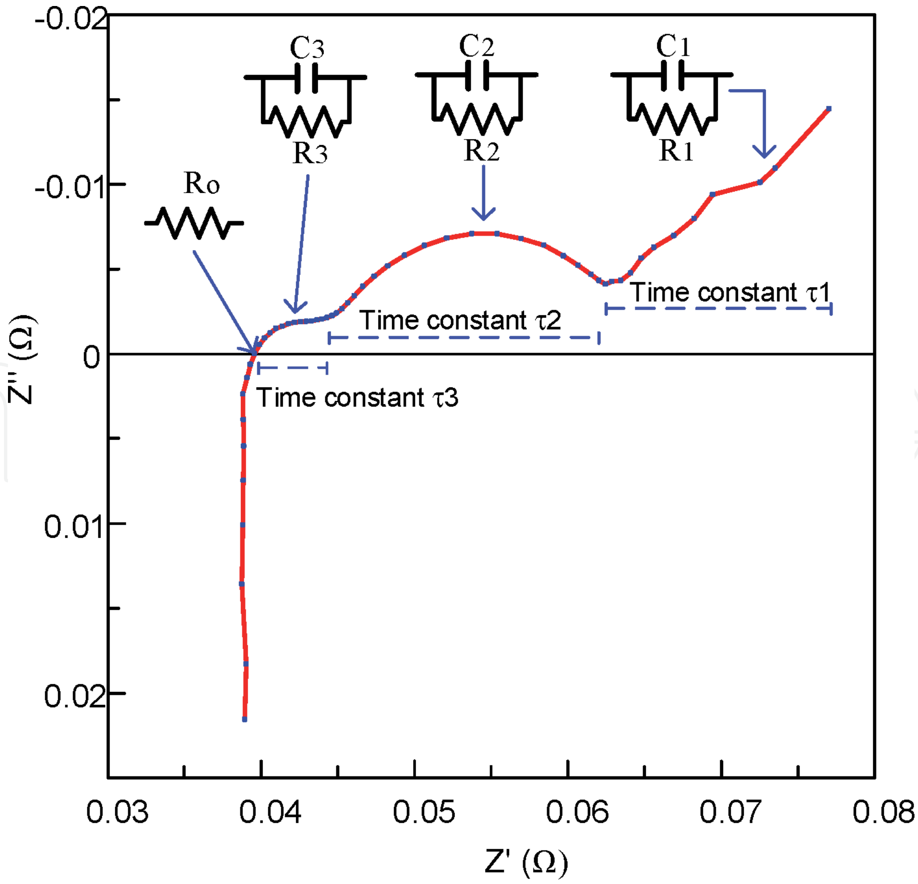


**Figure 6.**
*Time constants associated with pack impedance.*

(Z") parts of the impedance decrease with frequency, drawing a line with a slope of almost 45°. From 18 mHz to 4 Hz, the plots present semicircular shapes, whose diameter diminishes with increasing SOC. For medium frequencies (4 to 316 Hz), the impedance corresponds to a semicircle of constant diameter. To simulate these capacitive behaviors, several *RC* networks connected in series can be used [20, 21]. The value of equivalent resistance of the battery-pack is $R_o \cong 39$ mΩ.

To analyze the influence of the impedance components on the dynamic response of the battery-pack, **Figure 6** shows the EIS result at 40% SOC. The results analysis allows to associate the most relevant time constants with the impedance behavior of the battery-pack. Most of the dynamic applications of the batteries (load/frequency control or renewable generation support) have their time constants from 1 mHz to 316 Hz; for this reason, the inductive behavior can be neglected. In this frequency range, the *RC* networks that reproduce the impedance behavior can be used to determine the different time constants that affect the dynamic response of the tested battery-pack. These time constants ($\tau 1$, $\tau 2$, $\tau 3$) are calculated from EIS test results and presented in **Table 3**.

### 2.3 Hybrid model of the battery-pack

As a result of these combined time- and frequency-domain tests, an electrical circuit has been determined. Also, the model includes an integration current SOC estimator, to guarantee that the parameters of the electrical circuit simulate the dynamic behavior of the battery-pack for different SOC conditions, as shown in **Figure 7**. The inputs of the model are the initial value of SOC ($SOC_0$), the battery-pack capacity ($Cn$), and the current ($i_{pack}$). The output corresponds to the voltage response of the battery-pack ($u_{pack}$), which is calculated by Eq. (2), where $uRo$, $uc1$,

| Element | 20% SOC | 40% SOC | 60% SOC | 80% SOC | 90% SOC |
|---|---|---|---|---|---|
| *Ro (Ω)* | 0.039 | 0.039 | 0.039 | 0.039 | 0.039 |
| *τ1(C1//R1) (s)* | 23.40 | 18.43 | 15.71 | 11.39 | 10.92 |
| *τ2(C2//R2) (s)* | 0.295 | 0.188 | 0.136 | 0.116 | 0.106 |
| *τ3(C3//R3) (s)* | 0.0028 | 0.0030 | 0.0030 | 0.0029 | 0.0028 |

**Table 3.**
*Battery-pack impedance parameters.*

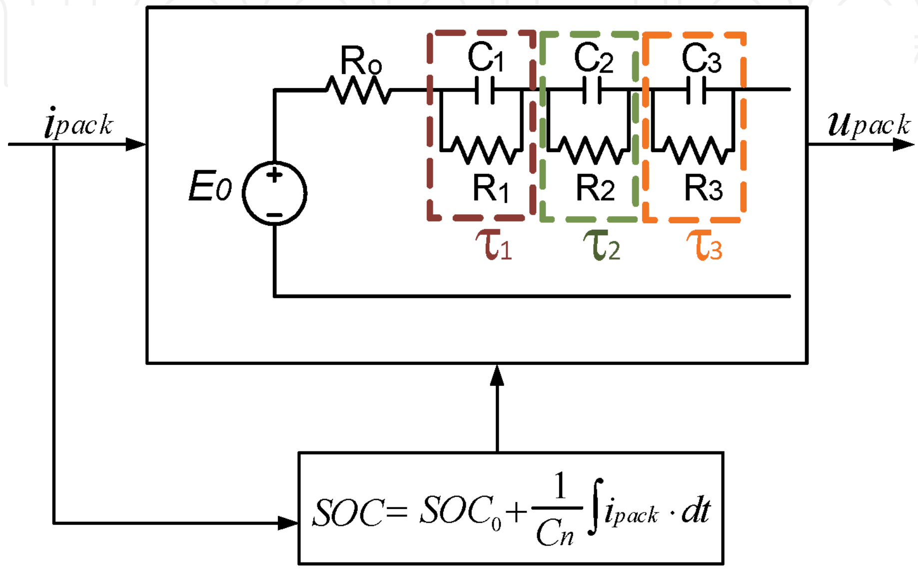


**Figure 7.**
*Battery-pack model.*

*uc2*, and *uc3* simulate the voltage response of the ohmic resistance and each *RC* network, respectively:

$$u_{pack}(SOC,t) = Eo(SOC,t) - u_{Ro}(SOC,t) - u_{C1}(SOC,t) - u_{C2}(SOC,t) - u_{C3}(SOC,t) \quad (2)$$

where:

$$u_{Ro}(SOC,t) = R_o(SOC)\cdot ipack(t) \quad (3)$$

$$u_{C1}(SOC,t) = \int \frac{1}{C_1(SOC)}\cdot\left(ipack(t) - \frac{u_{C1}(SOC)}{R_1(SOC)}\right)\cdot dt \quad (4)$$

$$u_{C2}(SOC,t) = \int \frac{1}{C_2(SOC)}\cdot\left(ipack(t) - \frac{u_{C2}(SOC)}{R_2(SOC)}\right)\cdot dt \quad (5)$$

$$u_{C3}(SOC,t) = \int \frac{1}{C_3(SOC)}\cdot\left(ipack(t) - \frac{u_{C3}(SOC)}{R_3(SOC)}\right)\cdot dt \quad (6)$$

## 3. Hybrid model validation

To verify the accuracy and reliability of the proposed model to simulate the battery-pack behavior, hardware-in-the-loop simulations are used. HIL is a widely used experimental technique to reproduce the real conditions of physical applications [27, 28], using lab devices such as electronic loads, power sources, sensors, and data acquisition systems (in the case of electric applications). To perform the HIL simulation of the battery-pack, the experimental setup shown in [26] is used. In this test bench, the load regime is simulated by means of a MATLAB/Simulink model (software simulation). This current signal is used to control (by DSpace control system) the output signal of an electronic load and a power source connected in parallel to reproduce the charging/discharging cycles. This configuration is called hardware simulation; in this way, real devices are used to test the battery-pack. A control schema of the HIL simulation is shown in **Figures 8** and **9** that presents a picture of the test bench.

Three simulations of the battery-pack performance under dynamic regimes associated with distribution grids operation have been analyzed. The first one corresponds to a load frequency control application (LFC), which is related to grid frequency control, with typical time constants ranging from 0.2 ms to 10 s. The second one reproduces the dynamic voltage support (DVS) of a renewable energy source during 110 s. The simulated models of these load regimes are based on the operation of a hybrid ac/dc microgrid presented in [29]. Finally, the third one simulates the performance of an energy support device uninterruptible power supply (UPS). The time duration of this energy support is less than 30 min; and to

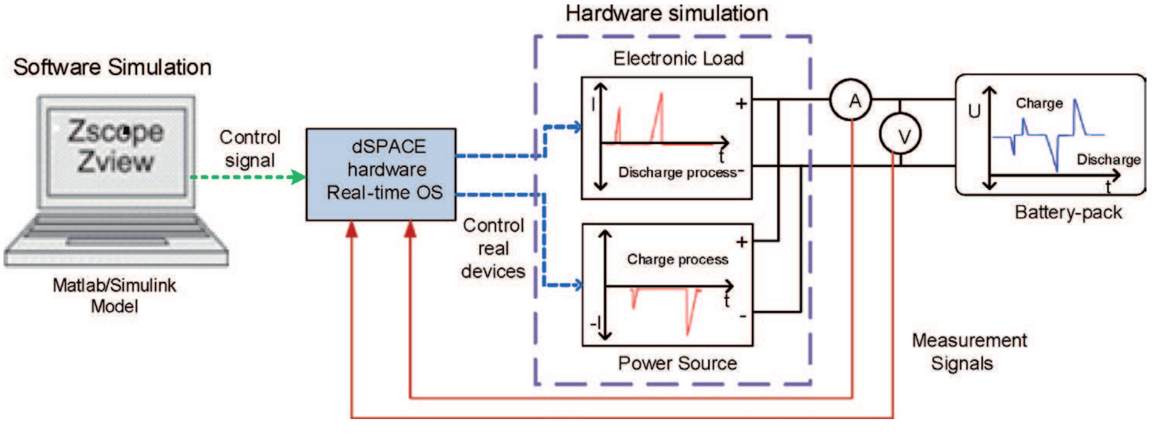


**Figure 8.**
*HIL simulation control setup.*

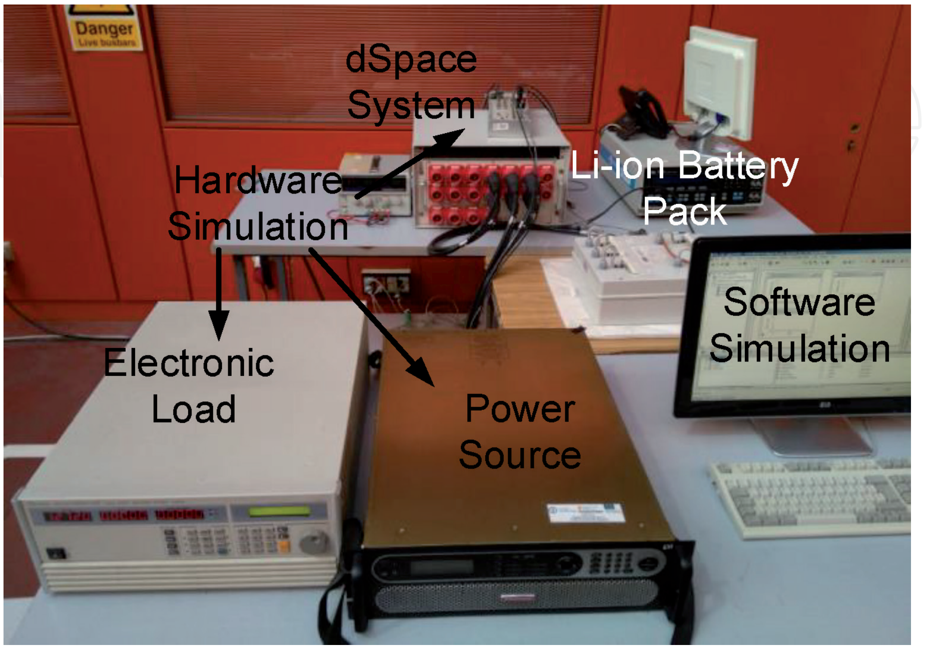


**Figure 9.**
*Test bench picture.*

test the transient response, different current steps have been simulated. The current profiles associated with these applications are shown in **Figures 10–12**. These current signals are used as the input signals of the HIL simulations. The simulations have been performed at different SOC values to check the model response under SOC variations. **Figures 13–18** present the comparison of the voltage response of the hybrid model ($U_{model}$) and the voltage measurement at battery-pack terminals ($U_{bpack}$) during the HIL simulations.

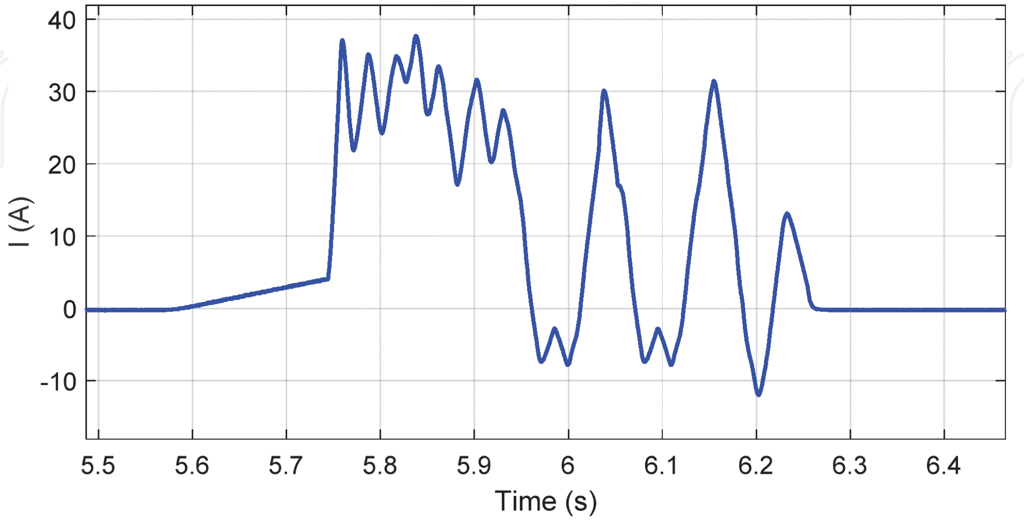


**Figure 10.**
*Current profile of LFC simulation.*

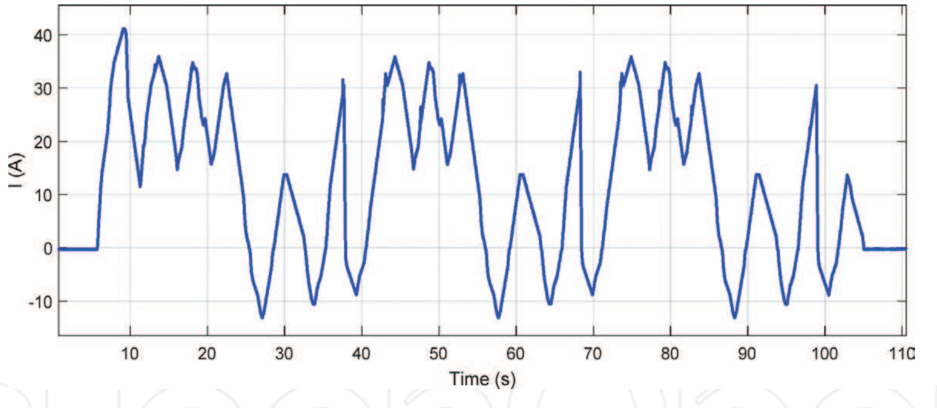


**Figure 11.**
*Current profile of DVS simulation.*

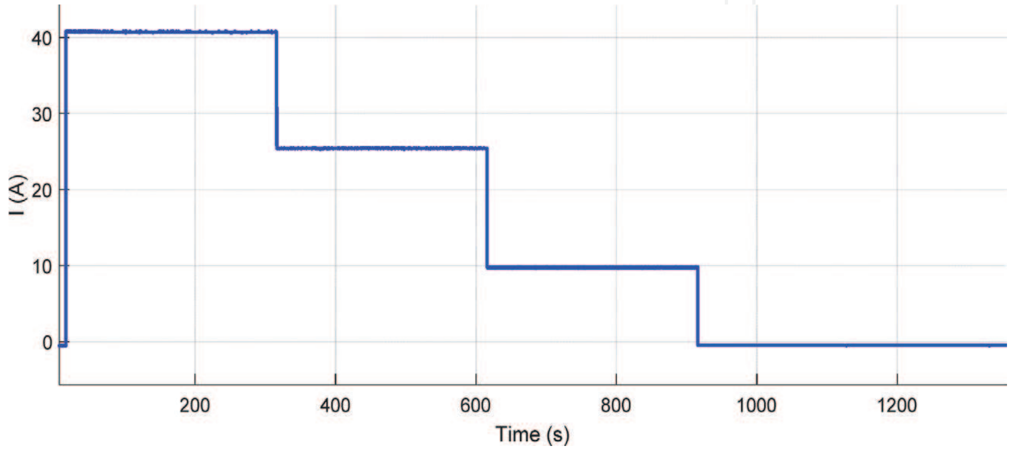


**Figure 12.**
*Current profile of UPS simulation.*

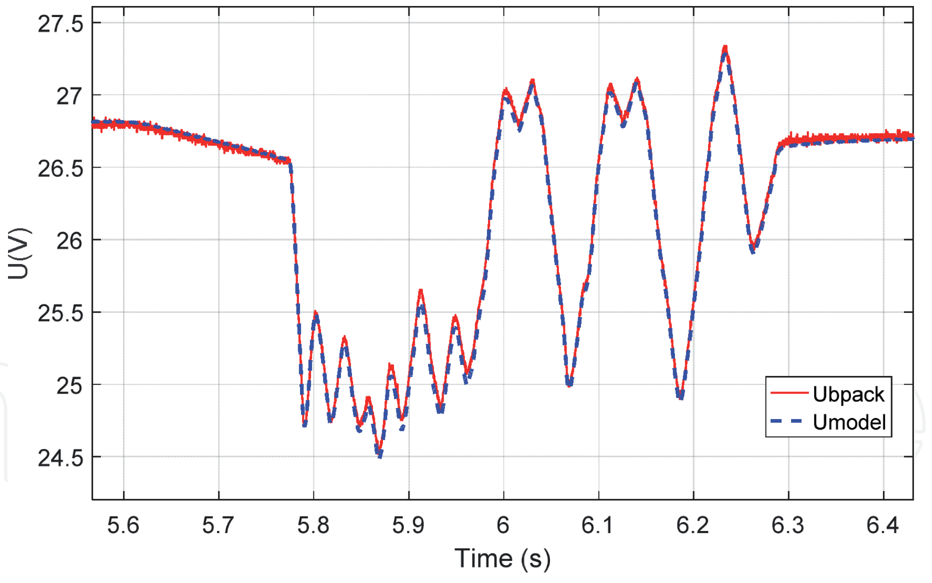


**Figure 13.**
*Simulation results at LFC (48% SOC).*

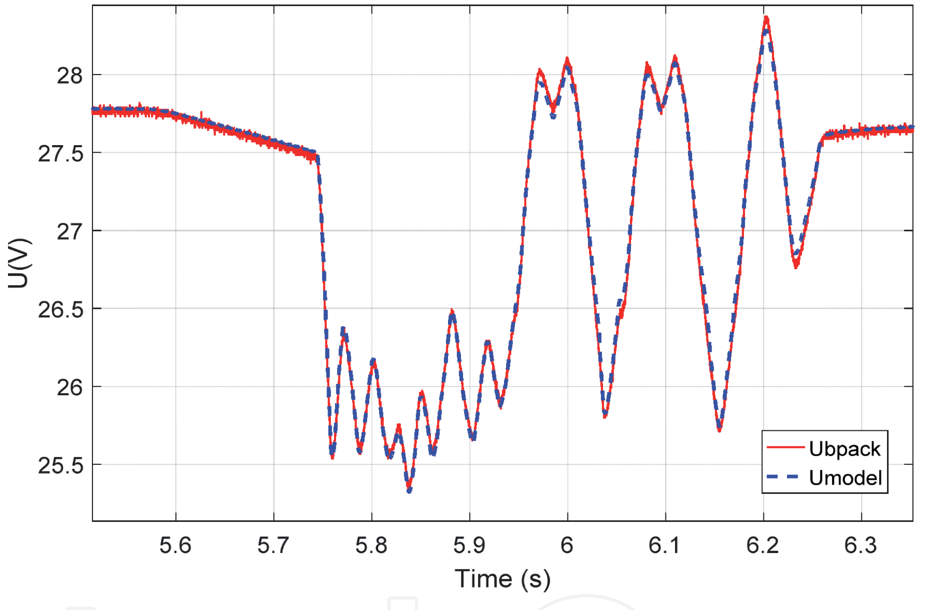


**Figure 14.**
*Simulation results at LFC (72% SOC).*

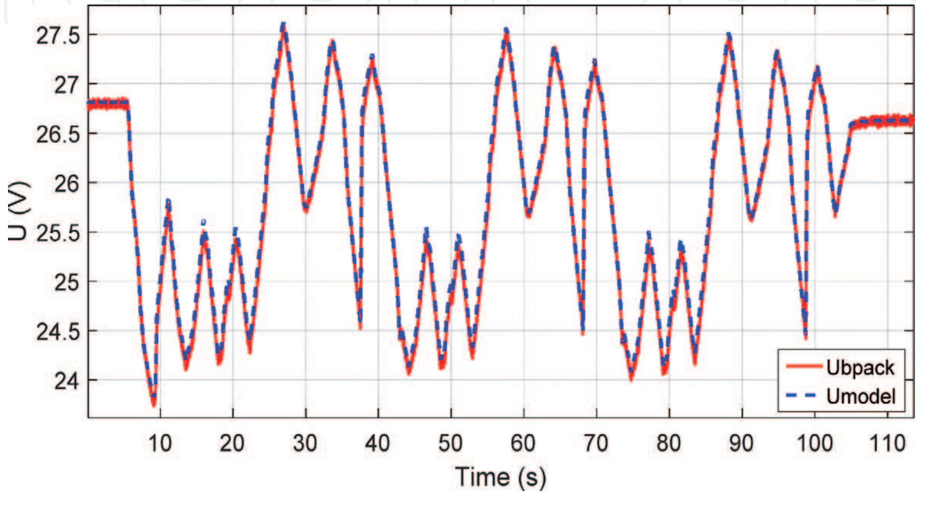


**Figure 15.**
*Simulation results at DVS (45% SOC).*

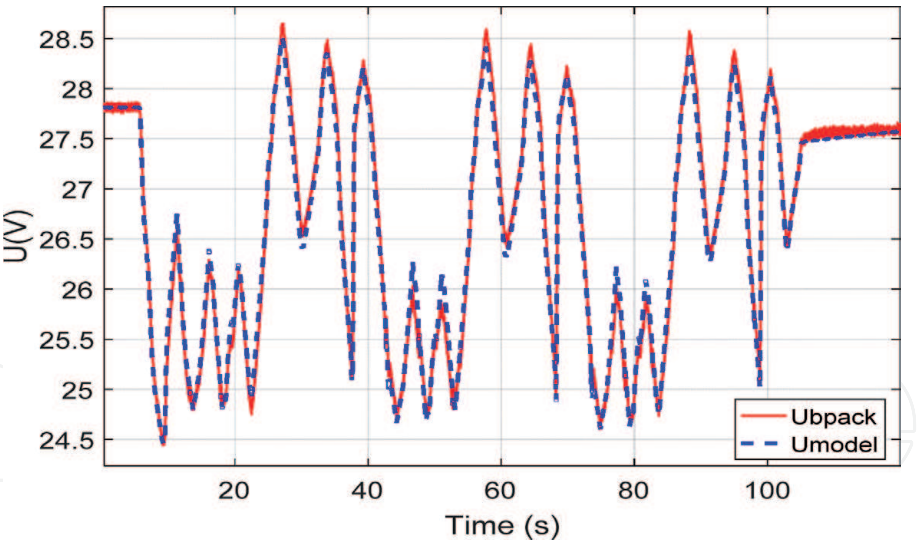


**Figure 16.**
*Simulation results at DVS (73% SOC).*

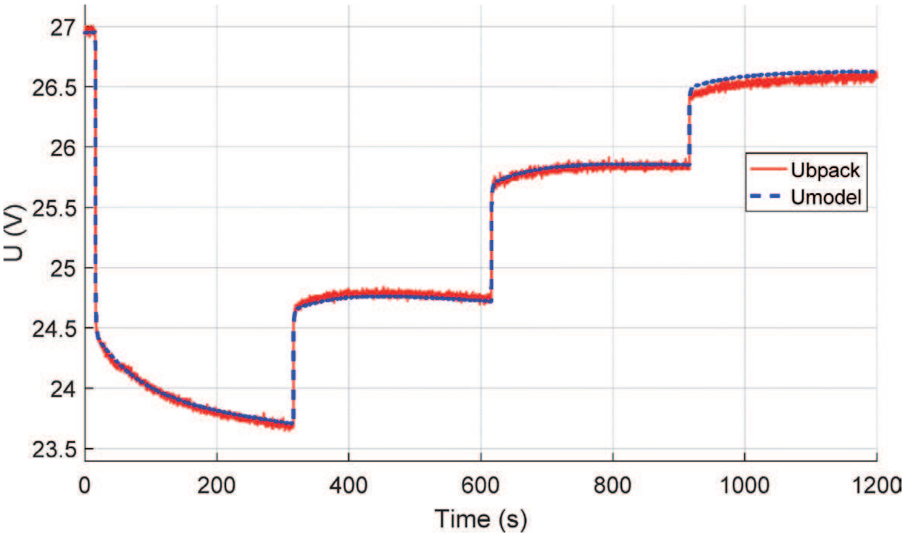


**Figure 17.**
*Simulation results at UPS (53% SOC).*

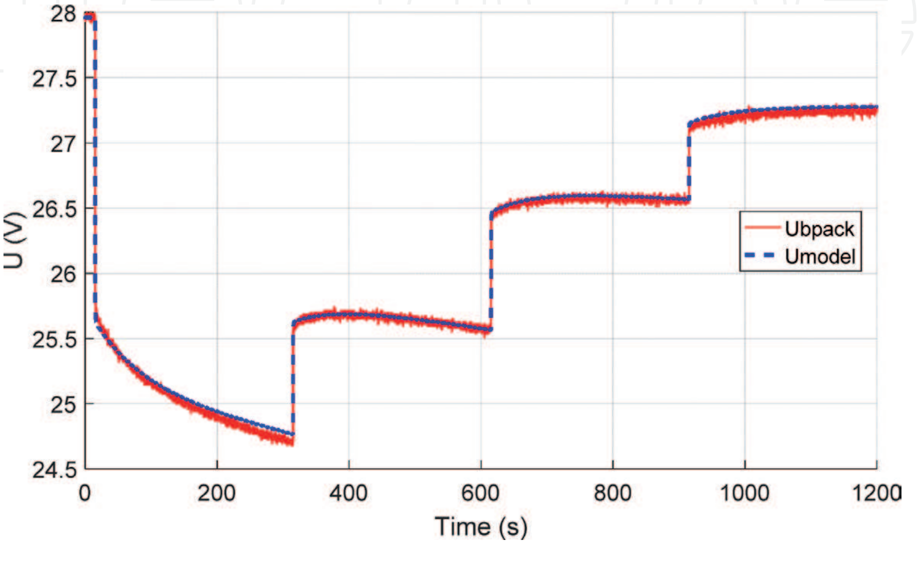


**Figure 18.**
*Simulation results at UPS (78% SOC).*

The validations tests show that the hybrid model simulates the battery-pack behavior with high accuracy in all cases analyzed. The maximum errors for each simulation are 0.28% (LFC), 0.40% (DVS), and 0.23% (UPS).

## 4. Conclusions

This chapter presents a hybrid modeling procedure of Li-ion battery-packs which is able to simulate the dynamic behavior associated with electric grid applications. The parameters of an electrical circuit have been calculated from experimental results of current interruption and EIS tests. The active behavior of the battery-pack has been simulated by a voltage source, and the impedance reflects the electrochemical processes by means of three *RC* networks (which correspond to three different time constants) and an ohmic resistance. The experimental procedure has been performed at the whole battery-pack in order to include the interactions of battery cells and BMS components.

To reproduce the battery-pack behavior under high dynamic applications of distribution grids, a hardware-in-the-loop platform has been used. Three different cases (load frequency control, dynamic voltage support, and uninterruptible power supply) at different SOC conditions have been simulated. The validation results show that the hybrid model reproduces the dynamic behavior of the battery-pack with high accuracy in all cases analyzed.

## Conflict of interest

The authors declare no conflict of interest.

## Author details

Sandra Castano-Solis[1*], Daniel Serrano-Jiménez[2], Jesús Fraile-Ardanuy[3], David Jiménez-Bermejo[3] and Javier Sanz-Feito[4]

1 ETS Ingeniería y Diseño Industrial, Universidad Politécnica de Madrid, Madrid, Spain

2 Electronic Engineering and Computation Science Department, Universidad de Mondragón, Guipúzcoa, Spain

3 ETSI Telecomunicación, Universidad Politécnica de Madrid, Madrid, Spain

4 Electrical Engineering Department, Universidad Carlos III de Madrid, Madrid, Spain

*Address all correspondence to: sp.castano@upm.es

## References

[1] Mohamad F, Teh J, Lai C-M, Chen L-R. Development of energy storage systems for power network reliability: A review. Energies. 2018;**11**(9):2278

[2] Hill CA, Such MC, Chen D, Gonzalez J, Grady WM. Battery energy storage for enabling integration of distributed solar power generation. IEEE Transactions on Smart Grid. 2012;**3**(2):850-857

[3] Luo X, Wang J, Dooner M, Clarke J. Overview of current development in electrical energy storage technologies and the application potential in power system operation. Applied Energy. 2015;**137**:511-536

[4] Abada S, Marlair G, Lecocq A, Petit M, Sauvant-Moynot V, Huet F. Safety focused modeling of lithium-ion batteries: A review. Journal of Power Sources. 2016;**306**:178-192

[5] Li S, Mi CC, Zhang M. A high-efficiency active battery-balancing circuit using multiwinding transformer. IEEE Transactions on Industry Applications. 2013;**49**:198-207

[6] Li J, Greye B, Buchholz M, Danzer MA. Interval method for an efficient state of charge and capacity estimation of multicell batteries. Journal of Energy Storage. 2017;**13**:1-9

[7] Hu Y, Yurkovich S, Guezennec Y, Yurkovich BJ. A technique for dynamic battery model identification in automotive applications using linear parameter varying structures. Control Engineering Practice. 2009;**17**(10):1190-1201

[8] Sikha G, White R, Popov B. A mathematical model for a lithium-ion battery/electrochemical capacitor hybrid system. Journal of the Electrochemical Society. 2005;**152**(8):A1682-A1693

[9] Smith K, Rahn C, Wang C. Model-based electrochemical estimation and constraint management for pulse operation of lithium ion batteries. IEEE Transactions on Control Systems Technology. 2010;**18**(3):654-663

[10] Shafiei A, Momeni A, Williamson S. Battery modeling approaches and management techniques for plug-in hybrid electric vehicles. In: Proceedings of Vehicle Power and Propulsion Conference, VPPC'11. 2011. pp. 1-5

[11] Abu-Sharkh S, Doerffel D. Rapid test and non-linear model characterization of solid-state lithium-ion batteries. Journal of Power Sources. 2004;**130**:266-274

[12] He H, Xiong R, Zhang X, Sun F, Fan J. State-of-charge estimation of the lithium-ion battery using an adaptive extended Kalman filter based on an improved Thevenin model. IEEE Transactions on Vehicular Technology. 2011;**60**(4):1461-1469

[13] Purvins A, Papaioannou IT, Debarberis L. Application of battery-based storage systems in household-demand smoothening in electricity-distribution grids. Energy Conversion and Management. 2013;**65**:272-284

[14] Chan HL, Sutanto D. A new battery model for use with battery energy storage systems and electric vehicles power systems. In: Proceedings of Power Eng Soc Winter Meet. 2000. pp. 470-475

[15] He H, Xiong R, Guo H, Li S. Comparison study on the battery models used for the energy management of batteries in electric vehicles. Energy Conversion and Management. 2012;**64**:113-121

[16] Zheng Y, Gao W, Ouyang M, Lu L, Zhou L, Han X. State-of-charge

inconsistency estimation of lithium-ion battery pack using mean-difference model and extended Kalman filter. Journal of Power Sources. 2018;**383**:50-58

[17] El Din MS, Abdel-Hafez MF, Hussein AA. Enhancement in Li-ion battery cell state-of-charge estimation under uncertain model statistics. IEEE Transactions on Vehicular Technology. 2016;**65**(6):4608-4618

[18] Andre D, Meiler M, Steiner K, Walz H, Soczka-Guth T, Sauer DU. Characterization of high-power lithium-ion batteries by electrochemical impedance spectroscopy. II: Modelling. Journal of Power Sources. 2011;**196**:5349-5356

[19] Castano S, Gauchia L, Sanz J. Effect of packaging on Supercapacitors string modeling: proposal of a functional unit defined around the balancing circuit. IEEE Transactions on Components, Packaging and Manufacturing Technology. 2013;**3**(8):1390-1398

[20] Buller S, Thele M, De Doncker RWAA, Karden E. Impedance-based simulation models of supercapacitors and Li-ion batteries for power electronic applications. IEEE Transactions on Industry Applications. 2005;**41**(3):742-747

[21] Karden E, Buller S, De Doncker RW. A frequency-domain approach to dynamical modeling of electrochemical power sources. Electrochimica Acta. 2002;**47**(13):2347-2356

[22] Castano-Solis S, Serrano-Jimenez D, Fraile-Ardanuy J, Sanz-Feito J. Hybrid characterization procedure of Li-ion battery packs for wide frequency range dynamics applications. Electric Power Systems Research. 2019;**166**:9-17

[23] Castano-Solis S, Serano-Jimenez D, Gauchia L, Sanz J. The influence of BMSs on the characterization and modeling of series and parallel Li-ion packs. Energies. 2017;**10**(3):273

[24] Jossen A. Fundamentals of battery dynamics. Journal of Power Sources. 2006;**154**(2):530-538

[25] Dai H, Wei X, Sun Z, Wang J, Gu W. Online cell SOC estimation of Li-ion battery packs using a dual time-scale Kalman filtering for EV applications. Applied Energy. 2012;**95**:227-237

[26] Castano-Solis S, Gauchia L, Serrano Jimenez D, Sanz Feito J. Off-the-shelf and flexible hybrid frequency and time domain experimental architecture setup for electrochemical energy modules testing under realistic operating conditions. IEEE Transactions on Energy Conversion. 2017;**32**(2):620-627

[27] Huerta F, Tello RL, Prodanovic M. Real-time power-hardware-in-the-loop implementation of variable-speed wind turbines. IEEE Transactions on Industrial Electronics. 2017;**64**(3):1893-1904

[28] Gauchia L, Sanz J. A per-unit hardware-in-the-loop simulation of a fuel cell/battery hybrid energy system. IEEE Transactions on Industrial Electronics. 2010;**57**(4):1186-1194

[29] Liu X, Wang P, Loh PC, Hybrid A. AC/DC microgrid and its coordination control. IEEE Transactions on Smart Grid. 2011;**2**(2):278-286